



About the performance of perturbative treatments of the spin-boson dynamics within the hierarchical equations of motion approach

Meng Xu^a  and Joachim Ankerhold^b

Institute for Complex Quantum Systems and IQST, Ulm University, Albert-Einstein-Allee 11, 89069 Ulm, Germany

Received 26 June 2023 / Accepted 3 October 2023 / Published online 11 October 2023
© The Author(s) 2023

Abstract The hierarchical equations of motion (HEOM) provide a numerically exact approach for simulating the dynamics of open quantum systems coupled to a harmonic bath. However, its applicability has traditionally been limited to specific spectral forms and relatively high temperatures. Recently, an extended version called Free-Pole HEOM (FP-HEOM) has been developed to overcome these limitations. In this study, we demonstrate that the FP-HEOM method can be systematically employed to investigate higher order master equations by truncating the FP-HEOM hierarchy at a desired tier. We focus on the challenging scenario of the spin-boson problem with a sub-Ohmic spectral distribution at zero temperature and analyze the performance of the corresponding master equations. Furthermore, we compare the memory kernel for population dynamics obtained from the exact FP-HEOM dynamics with that of the approximate Non-Interacting-Blip Approximation (NIBA).

1 Introduction

The second-order quantum master equation (QME) is a fundamental tool for studying the dynamics of open quantum systems and finds wide-ranging applications in diverse fields, including quantum optics, condensed matter physics, condensed phase chemistry, and biology [1–6]. However, employing the QME in regimes with strong non-Markovian behavior, characterized by slow environmental evolution and significant retardation effects on the subsystem, presents substantial challenges. These challenges become even more pronounced in low-temperature conditions and structured environments, where non-Markovian effects are amplified. A notable example is the unconventional impact of sub-Ohmic noise at zero temperature [7–11].

To address the limitations of the QME in handling pronounced non-Markovian retardation effects, incorporating higher order corrections that account for system-bath correlations becomes essential [12–14]. However, direct calculations involving these terms require computing high-dimensional time integrals, which is a daunting task [15, 16]. To the best of our

knowledge, analytical calculations of high-order perturbations or kernels have only been achieved up to the sixth order [17, 18]. Previous work has employed numerical techniques such as hierarchical equations of motion (HEOM) to compute higher order effects [13, 14]. However, these approaches have been primarily limited to elevated-temperature regimes due to the exponential increase in the number of auxiliary density operators (ADOs) involved, a challenge commonly referred to as the curse of dimensionality. This challenge becomes even more severe as the temperature approaches zero, making the analysis of memory kernels' properties and high-order perturbative master equations increasingly demanding.

To investigate the effects of high-order kernels in unconventional environments, we address key challenges such as zero-temperature calculations employing the widely used HEOM method [11, 13, 19–44]. The HEOM approach utilizes a set of ADOs to unravel system-bath correlations within an extended state space [26, 32, 33, 41, 45]. Conventionally, these ADOs are constructed as high-dimensional arrays based on a series of exponential functions derived from the decomposition of the bath correlation function. The extended space, expanded by ADOs, grows exponentially with the number of modes, posing significant challenges in scenarios involving low temperatures and structured bath spectra. This is particularly relevant as standard

^ae-mail: meng.xu@uni-ulm.de (corresponding author)

^be-mail: joachim.ankerhold@uni-ulm.de (corresponding author)

analytical Matsubara frequencies (i.e., $\nu_k = 2k\pi/\beta$) shift toward a continuum strip as temperatures decrease ($\beta = 1/T$). Therefore, developing an efficient method for obtaining a limited number of well-behaved modes becomes crucial for successfully implementing HEOM in the study of quantum master equations.

Several decomposition schemes [11, 43, 46] have been developed to address the limitations of HEOM in low-temperature and general spectral density scenarios, such as the frequency-domain barycentric spectrum decomposition (BSD) [11]. The effectiveness of these decomposition schemes has been demonstrated by their ability to reproduce phenomena like the Kondo resonance peak in Fermi baths [46] and the Shiba relation in sub-Ohmic boson baths [11]. Notably, by optimizing the properties of auxiliary modes under specific constraints, these schemes allow for the integration of a minimal number of modes (poles) into various versions of HEOM and other methods, such as the pseudomode approach [47], the hierarchy of pure states (HOPS) [48], and the nonequilibrium dynamical mean-field theory (DMFT) [49], even in unconventional environments.

In this work, we employ the Free-Poles HEOM (FP-HEOM) [11], which combines the optimized BSD and a hierarchical structure, to showcase the performance of higher order master equations in addressing unconventional environments. We also compare it with the well-established Non-Interacting-Blip Approximation (NIBA), a powerful but approximate scheme for non-perturbative treatment of the system-bath coupling in spin systems. The remainder of this paper is organized as follows: In Sections II and III, we provide a brief overview of the hierarchical equations of motion and discuss their limitations in simulating dynamics of open quantum systems. In Section IV, we present numerical simulation results to demonstrate the efficiency and accuracy of our proposed method. Finally, we summarize our findings and discuss potential avenues for future research in the concluding section.

2 Model Hamiltonian

The spin-boson model, which describes a two-state system interacting bilinearly with a harmonic bath, has been extensively studied in open quantum system dynamics [7]. In this work, we employ this model as a prototypical example to benchmark our method, while generalizations to more complex models are straightforward.

We consider a spin-boson model with the Hamiltonian

$$H_T = \epsilon\sigma_z + \Delta\sigma_x + \sum_i c_i x_i \sigma_z + \sum_i \left(\frac{p_i^2}{2m_i} + \frac{1}{2} m_i \omega_i^2 x_i^2 + \frac{1}{2} \mu \sigma_z^2 \right), \quad (1)$$

where the system degrees of freedom (DoF) are represented by dimensionless Pauli matrices σ_x and σ_z . Δ and 2ϵ denote the tunneling energy and energy bias between the two eigenstates of σ_z , i.e., $|\pm\rangle$. The i th harmonic modes of the reservoir is characterized by its mass, coordinate, momentum, and frequency, i.e., m_i , x_i , p_i , and ω_i , respectively. The coupling between the system and the i th bath mode is denoted by c_i with $[m\omega^2x]$ dimension.

The effective impact of the bath on the system is fully described by the coupling-weighted spectral density

$$J(\omega) = \frac{\pi}{2} \sum_i \frac{c_i^2}{m_i \omega_i} \delta(\omega - \omega_i). \quad (2)$$

In the following, we assume a generic spectral density [50] of the form

$$J(\omega) = \frac{\pi}{2} \alpha \omega_c^{1-s} \omega^s e^{-\omega/\omega_c}, \quad (3)$$

where α is the dimensionless Kondo parameter characterizing the system-bath dissipation strength and ω_c is the characteristic frequency of the bath. For $s = 1$, this spectral distribution describes an ohmic reservoir and it is called sub-ohmic for $s < 1$. In the latter situation, the interplay of the relatively large portion of low-frequency modes with the internal two-level dynamics makes this model extremely challenging to simulate, particularly in the long time limit and close to or at $T = 0$.

3 Hierarchical equations of motion

We briefly describe the essence of the HEOM approach and refer to the literature for further details. The derivation assumes a factorized initial states of the total density at time zero, i.e., $W(0) = \rho_s(0) \otimes e^{-\beta H_b} / \text{Tr} e^{-\beta H_b}$. The generalization to correlated initial states can be found in Refs. [51, 52].

In path integral representation [53], a formally exact expression for the reduced density is obtained by integrating over the bath degrees of freedom. The effective impact of the bath onto the system dynamics is captured by the Feynman–Vernon influence functional [53] which reads

$$\mathcal{F}[q^+, q^-] = - \int_0^t ds \int_0^s d\tau [q^+(s) - q^-(s)] \times [C(s - \tau)q^+(\tau) - C^*(s - \tau)q^-(\tau)]. \quad (4)$$

In the expression above, the forward and backward paths of the subsystem, denoted by $q^\pm(\tau)$, are defined through the relation

$$q^\pm(\tau) = \langle q^\pm(\tau^+) | \sigma_z | q^\pm(\tau) \rangle, \quad (5)$$

where $|q^\pm\rangle$ represent the eigenstates of σ_z , and τ^+ signifies the moment immediately following the time slice τ . The influence functional describes arbitrary long-ranged self-interactions in time of the system paths determined by the bath auto-correlation $C(t) = \langle \xi(t)\xi(0) \rangle$ with the collective degree of freedom $\xi = \sum_i c_i x_i$. Particularly at low temperatures, correlation functions are known to decay algebraically, so that direct simulations of the path integral, e.g., via path integral Monte Carlo (PIMC) [10, 54], are plagued by a degrading signal-to-noise ratio.

The hierarchical equations of motion (HEOM) approach deals with this problem by converting the time-non-local path integral into a set of time-local differential equations through the introduction of auxiliary density operators (ADOs). The basic ingredient is a decomposition of $C(t)$ in a series of K exponential modes, where K has to be sufficiently bounded for the nested hierarchy to be practically solvable. To formulate a minimal set of modes is thus the prerequisite to access low temperatures and long times. As a matter of fact, this problem has been solved by us only recently [11] by implementing the barycentric representation of rational functions for the spectral noise power $S_\beta(\omega)$, i.e., the Fourier transform of $C(t)$

$$C(t) = \frac{1}{\pi} \int_{-\infty}^{+\infty} d\omega S_\beta(\omega) e^{-i\omega t} = \sum_{k=1}^K d_k e^{-z_k t} + \delta C(t) \quad t \geq 0 \tag{6}$$

with complex-valued amplitudes d_k and frequencies $z_k = \gamma_k + i\omega_k$, $\gamma_k > 0$. Here, $S_\beta(-\omega)$ and $S_\beta(\omega)$ are related by the fluctuation dissipation theorem which can be cast into the form $S_\beta(\omega) = 2[n_\beta(\omega) + 1]J(\omega)$ with the Bose distribution $n_\beta(\omega) = 1/[\exp(\beta\omega) - 1]$. The barycentric representation constructs a function $\tilde{S}_\beta(z)$ in the complex plane, such that it is along the real axis an approximant of $S_\beta(\omega)$ (AAA algorithm, see [55]). The poles and the residues of \tilde{S}_β appear as $\{d_k\}$ and $\{z_k\}$ in (6). For details of this Free-Pole HEOM, see [11, 56]. One can show that the FP-HEOM thus operates with a minimal set of K modes with the correction $\delta C(t)$ below a chosen threshold.

The exponential function’s self-derivative property in (6) then allows to ‘unravel’ the time non-locality of the original Feynman–Vernon path integral by introducing ADOs $\rho_{\mathbf{m},\mathbf{n}}(t)$ with multi-indices $\mathbf{n} = (n_1, \dots, n_K)$ and $\mathbf{m} = (m_1, \dots, m_K)$. This then leads to a nested hierarchy of time-local evolution equations for the ADOs, that is

$$\dot{\rho}_{\mathbf{m},\mathbf{n}} = - \left(i\mathcal{L}_s + \sum_{k=1}^K m_k z_k + \sum_{k=1}^K n_k z_k^* \right) \rho_{\mathbf{m},\mathbf{n}} - i \sum_{k=1}^K \sqrt{(m_k + 1) d_k} \left[\hat{q}, \hat{\rho}_{\mathbf{m}_k^+, \mathbf{n}} \right]$$

$$- i \sum_{k=1}^K \sqrt{(n_k + 1) d_k^*} \left[\hat{q}, \hat{\rho}_{\mathbf{m}, \mathbf{n}_k^+} \right] - i \sum_{k=1}^K \sqrt{m_k d_k} \hat{q} \hat{\rho}_{\mathbf{m}_k^-, \mathbf{n}} + i \sum_{k=1}^K \sqrt{n_k d_k^*} \hat{\rho}_{\mathbf{m}, \mathbf{n}_k^-} \hat{q}. \tag{7}$$

The subscript \mathbf{m}_k^\pm and \mathbf{n}_k^\pm denote $\{m_1, \dots, m_k \pm 1, \dots, m_K\}$ and $\{n_1, \dots, n_k \pm 1, \dots, n_K\}$, respectively. The bare system evolution is propagated by $\mathcal{L}_s \rho = [H_s, \rho]$. Eventually, the physical reduced density matrix $\hat{\rho}_s$ corresponds to the multi-index $\mathbf{m} = \mathbf{n} = 0$. To boost the numerical efficiency of the FP-HEOM (7), matrix product state (MPS) representations can be conveniently implemented which allows to tackle also asymptotic times down to temperature zero [11].

Note that truncating the nested hierarchy of ADOs after the L^{th} tier, as given by

$$\sum_k (n_k + m_k) \leq L, \tag{8}$$

implies the inclusion of system-bath coupling strengths up to the order of α^{2L} [57]. Indeed, as demonstrated in previous works [58–60], truncating at $L = 1$ yields a generalized Redfield equation.

4 Numerical results

In this section, we employ the non-perturbative Free-Pole Hierarchical Equations of Motion (FP-HEOM) method to study the dynamics of a two-level quantum system coupled to a sub-Ohmic bosonic bath. We consider bath temperatures ranging from $T = 0$ to finite $T \neq 0$, with a spectral density $J(\omega) \propto \omega^s$ where $0 \leq s \leq 1$. Our analysis focuses on three key aspects: (i) The convergence properties of higher order master equations concerning the system-bath coupling strength α and spectral exponent s . (ii) The accuracy of the Redfield-plus equation (12) across diverse temperature and bias regimes. (iii) The role of non-perturbative memory kernels as effective generators for system dynamics.

To ensure the accuracy of our results, we employed a barycentric decomposition with a stringent tolerance threshold defined by $\delta C(t) \leq 10^{-6}$, where $\delta C(t)$ represents the time-dependent deviation of the computed correlation function. The FP-HEOM equations were propagated using the Time-Dependent Variational Principle (TDVP) [61], represented using Matrix Product States (MPS) [27]. It is noteworthy that the bond dimension, χ of MPS exhibits an inverse relationship with the parameter s . Through meticulous optimization tests, we ascertained that for $s = 0$, a bond dimension

of $\chi = 50$ is optimal, whereas $s = 1$ is best represented with $\chi = 2$. All simulations were executed on a single core of an Intel Xeon Gold 6252 CPU clocked at 2.1 GHz. The computational durations varied, spanning from mere minutes to several hours, contingent on the specific scenario being analyzed.

4.1 Performance of truncated time-evolution equations within FP-HEOM

A variety of approximate methods for open quantum dynamics have been proposed, with the most notable ones considering the system-reservoir coupling up to the second order. When there is a clear separation in time scales between the rapid decay of reservoir correlations and the relaxation dynamics of the reduced density operator, these methods yield the Redfield master equation [62]. As highlighted earlier, an extended version of the Redfield equation, termed “Redfield-plus”, emerges naturally when the FP-HEOM is restricted to ADOs satisfying $\sum_k (n_k + m_k) \leq 1$. Specifically, in the interaction picture, the ADOs of the zeroth tier (reduced density matrix) are given by

$$\dot{\hat{\rho}}^I(t) = -i \sum_k [\hat{q}^I(t), \sqrt{d_k} \rho_{\mathbf{0}_k^+, \mathbf{0}}^I(t) + \sqrt{d_k^*} \rho_{\mathbf{0}, \mathbf{0}_k^+}^I(t)] \quad (9)$$

with the first-tier ADOs determined via

$$\frac{d}{dt} \hat{\rho}_{\mathbf{0}_k^+, \mathbf{0}}^I(t) = -z_k \rho_{\mathbf{0}_k^+, \mathbf{0}}^I(t) - i \sqrt{d_k} \hat{q}^I(t) \hat{\rho}_{\mathbf{0}, \mathbf{0}}^I(t); \quad (10a)$$

$$\frac{d}{dt} \hat{\rho}_{\mathbf{0}, \mathbf{0}_k^+}^I(t) = -z_k^* \rho_{\mathbf{0}, \mathbf{0}_k^+}^I(t) - i \sqrt{d_k^*} \hat{\rho}_{\mathbf{0}, \mathbf{0}}^I(t) \hat{q}^I(t). \quad (10b)$$

Here, the index I indicates the interaction picture. It is worth noting that the structure of Eqs. (9) and (10) resembles the one known from generalized Floquet theory for driven systems [63–65]. The factorized initial state gives a boundary condition with $\hat{\rho}_{\mathbf{0}, \mathbf{0}}^I(0) = \hat{\rho}(0)$ and all ADOs with $L > 0$ are set to zero.

The inhomogeneous differential equations in Eqs. (10) can be formally solved

$$\hat{\rho}_{\mathbf{0}_k^+, \mathbf{0}}^I(t) = -i \sqrt{d_k} \int_0^t d\tau e^{-z_k(t-\tau)} \hat{q}^I(\tau) \hat{\rho}_{\mathbf{0}, \mathbf{0}}^I(\tau); \quad (11a)$$

$$\hat{\rho}_{\mathbf{0}, \mathbf{0}_k^+}^I(t) = -i \sqrt{d_k^*} \int_0^t d\tau e^{-z_k^*(t-\tau)} \hat{\rho}_{\mathbf{0}, \mathbf{0}}^I(\tau) \hat{q}^I(\tau). \quad (11b)$$

and then plugged in into Eq. (9). Summation over the reservoir modes as in Eq. (6) then leads to the following time-evolution equation in Born approximation:

$$\frac{d}{dt} \hat{\rho}^I(t) = - \int_0^t d\tau [\hat{q}^I(t), C(t-\tau) \hat{q}^I(\tau) \rho^I(\tau)]$$

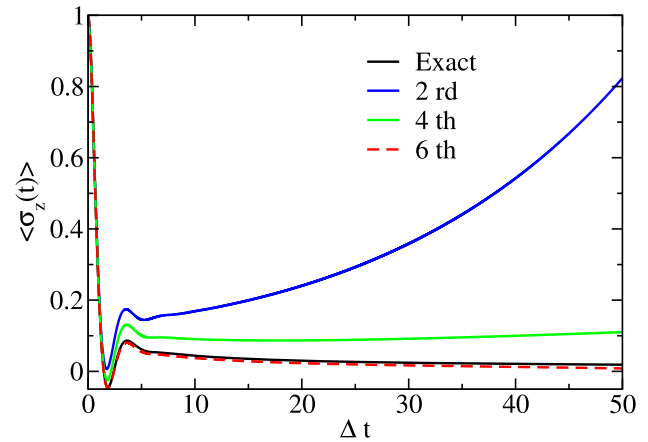


Fig. 1 Comparison of high-order perturbative time-evolution equations at tier L of FP-HEOM with fully converged simulations. The population dynamics of a sub-Ohmic spin-boson model are shown. Simulation parameters: $\epsilon = 0$, $\Delta = 1$, $\omega_c = 20$, $T = 0$, $\alpha = 0.1$, and $s = 0.5$

$$- [\hat{q}^I(t), C^*(t-\tau) \rho^I(\tau) \hat{q}^I(\tau)] \quad (12)$$

Note that no Markovian coarse-graining in time is done here, not even on the level of the reduced density so that the reservoir induced retardation is fully taken into account in this order of system-bath coupling. One regains the conventional Redfield equation by setting $\rho^I(\tau) \rightarrow \rho^I(t)$, thus leading to a time-local evolution equation with time-dependent rates. Hence, we name the above integro-differential equation (12) *Redfield-plus*.

The FP-HEOM can be interpreted as an infinite-order extension of the Redfield-plus/Redfield approximation [57, 66]. Truncating at tier L results in a time-evolution equation of order α^{2L} that’s non-local in time. This approach offers a systematic way to analyze the influence of higher order system-reservoir correlations, which can be intricate within a perturbative framework.

As illustrated in Fig. 1 for a coupling strength of $\alpha = 0.1$, numerically converged “exact” results are attainable when truncating at tier $L = 12$. However, the spin dynamics can be reasonably approximated at the 6th order ($L = 3$). The Redfield-plus approximation ($L = 1$) tends to diverge over extended time intervals. It is worth noting that while the FP-HEOM can handle strong system-bath couplings, in this context, we have selected a relatively weak parameter α to align with the perturbation series concept.

4.2 Redfield-plus: influence of low-frequency modes

Environment engineering in open quantum systems [67] focuses on the deliberate design and manipulation of a quantum system’s environment to induce specific dynamics, ranging from Markovian to non-Markovian or from delocalization to localization. Such strategies are invaluable for counteracting the adverse effects of decoherence and noise, two persistent challenges in

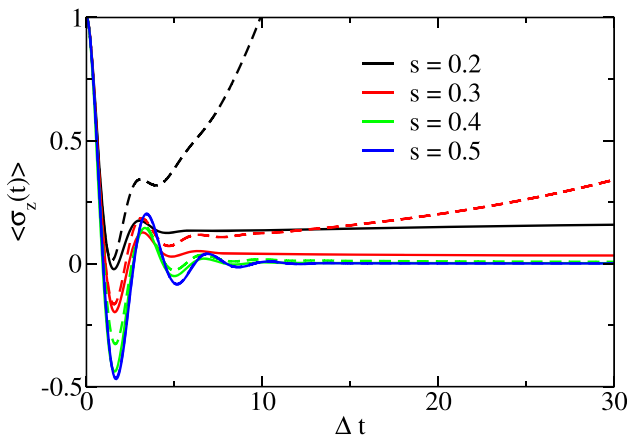


Fig. 2 Comparison of Redfield-plus (dashed line) with exact simulations (solid line) across varying spectral exponents s for a sub-ohmic spin-boson model. The depicted population dynamics utilize the following simulation parameters: $\epsilon = 0$, $\Delta = 1$, $\omega_c = 20$, $T = 0$, and $\alpha = 0.05$

quantum systems. In this section, we investigate the consequences of modulating the environmental spectrum through the parameter s on the dynamics of the subsystem.

For a sub-ohmic bosonic bath, the mode distribution, characterized by the spectral exponent s , is instrumental in gauging the efficacy of the Redfield-plus perturbative expansion. With a fixed coupling strength of $\alpha = 0.05$, Fig. 2 showcases that the Redfield-plus approximation closely mirrors the exact dynamics when the spectral exponents s are at least 0.5. However, as s diminishes, thereby accentuating the low-frequency modes, the precision of the second-order approximation wanes over incrementally shorter time intervals.

A decline in s within the sub-ohmic spectral density augments the spectral prominence of the low-frequency modes. This heightened influence of low-frequency modes undermines coherence by instigating extended temporal correlations, culminating in reservoir-dressed equilibrium states. Such dynamics have been previously observed, for example, in imaginary time path integral Monte Carlo simulations [9]. This intricate behavior underscores the limitations of a purely perturbative approach [7].

4.3 Redfield-plus: accuracy with respect to temperature and bias

In the high-temperature regime, the behavior of the effective noise spectral density at low frequencies becomes especially relevant. As the inverse temperature β (with $\beta = 1/(kT)$, where k is the Boltzmann constant, T is the temperature) approaches zero, and the noise spectral density $S_\beta(\omega)$ converges to

$$\begin{aligned} \lim_{\beta \rightarrow 0} S_\beta(\omega) &= \lim_{\beta \rightarrow 0} \frac{\frac{\pi}{2} \alpha \omega_c^{1-s} \omega^s e^{-\omega/\omega_c}}{1 - e^{-\beta\omega}} \\ &= \frac{\pi\alpha}{2\beta} \omega_c^{1-s} \omega^{s-1} e^{-\omega/\omega_c}. \end{aligned} \tag{13}$$

This limit implies an increase in the effective system-bath coupling as the temperature rises. This is a regime where the Redfield-plus approximation may fail, as illustrated in Fig. 3.

Figure 4 investigates the impact of bias on subsystem dynamics. As the bias escalates, the system transitions from a coherent to a decoherent state. Remarkably, under these conditions, the Redfield-plus approximation provides a reasonably accurate representation of the dynamics, as depicted in Fig. 4.

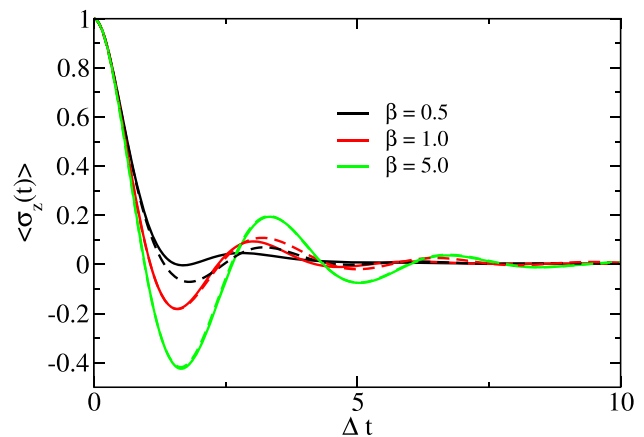


Fig. 3 Comparison of Redfield-plus (dashed line) and exact simulations (solid line) for a sub-ohmic spin-boson model at finite temperature. The simulation parameters are set as follows: $\epsilon = 0$, $\Delta = 1$, $\omega_c = 20$, and $\alpha = 0.05$

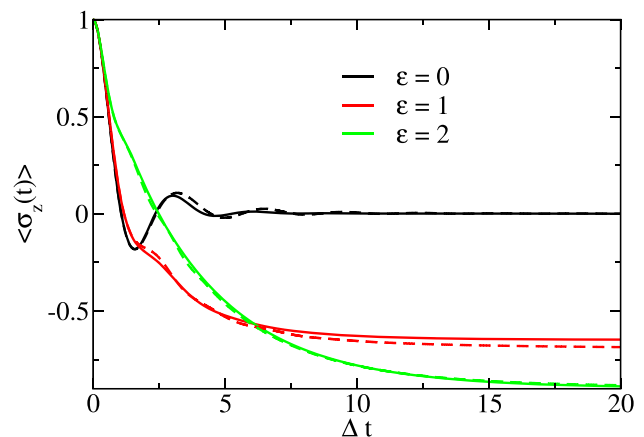


Fig. 4 Comparison of Redfield-plus (dashed line) and exact simulations (solid line) for a sub-ohmic biased spin-boson model at finite temperature. The simulation parameters are set as follows: $\Delta = 1$, $\omega_c = 20$, $\alpha = 0.05$, and $\beta = 1$

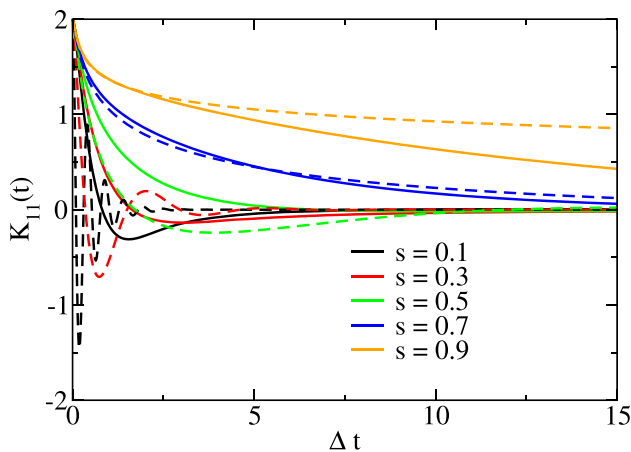


Fig. 5 Comparison of NIBA (dashed line) and exact simulations (solid line) for a sub-ohmic spin-boson model, illustrating the impact of varying the spectral exponent s on the memory kernel. Parameters: $\epsilon = 0$, $\Delta = 1$, $\omega_c = 20$, $\alpha = 0.05$, and $T = 0$

4.4 Time-dependent memory kernel for populations: NIBA versus FP-HEOM

For a spin system with no bias, i.e., $\epsilon = 0$, immersed in a bosonic bath, the expectation is that the steady-state population is uniformly distributed between the two spin states, i.e., $P(t \rightarrow \infty) = \langle \sigma_z(t \rightarrow \infty) \rangle \rightarrow 0$. However, it is well known that at zero temperature, a symmetry breaking can take place corresponding to a quantum phase transition from a delocalized to localized asymptotic state [10, 11]. Consequently, depending on the initial condition and reservoir parameters, $P(t) \neq 0$ over long timescales, which is a purely quantum phenomenon due to the absence of thermal fluctuations at zero temperature.

This behavior can be conveniently analyzed using the time-dependent memory kernel $K(t)$ which determines the spin dynamics according to

$$\dot{P}_\sigma(t) = - \sum_{\sigma'=\pm} \int_0^t d\tau K_{\sigma,\sigma'}(t-\tau) P_{\sigma'}(\tau). \quad (14)$$

We mention here that a powerful perturbative treatment to derive the kernel is the so-called Non-interacting Blip Approximation (NIBA) [7, 68] and its extensions. There, kernels in powers of the tunnel splitting Δ are obtained with the NIBA kernel being of second order in the tunnel splitting Δ^2 . Accordingly, the NIBA is not based on a series expansion in α and thus accounts also for strong spin-bath coupling. It neglects long-range quantum coherences though and does not predict the correct equilibrium state for $\epsilon \neq 0$. In Fig. 5 results for the NIBA memory kernel are depicted. From these data, one would conclude a change in the dynamical behavior (monotonous decay versus oscillatory decay) to occur for values around $s = 0.5$.

For smaller exponents, strong oscillations emerge with decreasing s .

In contrast, exact FP-HEOM data extracted from the exact dynamics [14] are shown in Fig. 5. For the chosen coupling strength, it is also observed that for $s > 0.5$, the memory decays clearly monotonous over time and remains always positive as also predicted by NIBA. However, quantitatively the exact decay appears to be much faster than within NIBA. For values of s below this threshold oscillatory pattern are seen as well for the FP-HEOM results, but with much smoother and with less oscillations as the NIBA prediction. We can thus conclude that while the NIBA provides qualitatively the correct physics, it is quantitatively in this regime of parameter space not reliable.

Physically, the changeover in dynamical behavior in $K(t)$ can be attributed to a freezing of the population, since the total weight of the kernel tends toward zero when integrated over a time span where $P_\sigma(t)$ does not change considerably. More specifically, in this regime of sufficiently small s , one may write for long times with $P_\sigma(\tau) \approx P_\sigma(t)$ in Eq. (14) that

$$\lim_{t \rightarrow \infty} \dot{P}_\sigma(t) \approx - \sum_{\sigma'=\pm} k_{\sigma,\sigma'} P_{\sigma'}(t) \quad (15)$$

with rates

$$k_{\sigma,\sigma'} = \int_0^\infty d\tau K_{\sigma,\sigma'}(\tau). \quad (16)$$

Estimations from Fig. 5 allow to see that rates $k_{\sigma,\sigma'}$ tend indeed to zero corresponding to a slowing down of the relaxation dynamics up to the regime, where $k_{\sigma,\sigma'} = 0$, so that the spin requires an infinitely long time to reach a Gibbs equilibrium state and instead displays localization. This property aligns with the fact that hybridization between spin and reservoir induced by slow modes occurs, thus freezing the spin dynamics.

5 Conclusion

Since conventional second-order master equations fail in accurately capturing non-Markovian dynamics, this limitation becomes markedly significant for unconventional baths, particularly in conditions such as zero-temperature structured environments. One approach to circumvent this is to incorporate high-order corrections. However, the numerical computation of high-dimensional integrals in time poses considerable challenge as the accuracy of calculations become extremely sensitive to numerical errors.

In this work, we have employed the Hierarchical Equations of Motion (HEOM) approach to effectively address these challenges. This methodology enables the systematic unraveling of higher order master equations, balancing numerical efficiency with high precision. Consequently, our investigation has concentrated on the

zero-temperature sub-Ohmic regimes, providing relevant computations to underscore our approach.

Furthermore, it is significant to note that the exact memory kernels in the quantum master equation can be extracted from the FP-HEOM approach and then be compared with those from perturbative schemes such as the NIBA. The extraction further offers a useful tool for the analysis of quantum phase transition dynamics, establishing a comprehensive and reliable platform for further explorations into open quantum system dynamics.

Acknowledgements The authors would like to thank Jiajun Ren, Haobin Wang, Frithjof B. Anders, and Matthias Vojta for sharing us their data as well as the fruitful discussions. M. X. acknowledges support from the state of BadenWürttemberg through bwHPC (JUSTUS 2). This work has been supported by the IQST, the German Science Foundation (DFG) under AN336/12-1 (For2724), the State of Baden-Württemberg under KQCBW/SiQuRe, the BadenWürttemberg Foundation within QT.BW (CDIN-QUA), and the BMBF through QSolid.

Funding Open Access funding enabled and organized by Projekt DEAL.

Data availability statement The data that support the figures within this article are available from the corresponding author upon reasonable request.

Open Access This article is licensed under a Creative Commons Attribution 4.0 International License, which permits use, sharing, adaptation, distribution and reproduction in any medium or format, as long as you give appropriate credit to the original author(s) and the source, provide a link to the Creative Commons licence, and indicate if changes were made. The images or other third party material in this article are included in the article's Creative Commons licence, unless indicated otherwise in a credit line to the material. If material is not included in the article's Creative Commons licence and your intended use is not permitted by statutory regulation or exceeds the permitted use, you will need to obtain permission directly from the copyright holder. To view a copy of this licence, visit <http://creativecommons.org/licenses/by/4.0/>.

References

1. C.W. Gardiner, P. Zoller, *Quantum Noise: A Handbook of Markovian and non-Markovian Quantum Stochastic Methods with Applications to Quantum Optics*, 3rd edn. (Springer, Berlin, 2004)
2. M.O. Scully, M.S. Zubairy, *Quantum Optics* (Cambridge University Press, Cambridge, 1997). <https://doi.org/10.1017/CBO9780511813993>
3. A. Kamenev, *Field Theory of Non-equilibrium Systems* (Cambridge University Press, Cambridge, 2023)
4. A. Nitzan, *Chemical Dynamics in Condensed Phases* (Oxford University Press, New York, 2006)
5. V. May, O. Kühn, *Charge and Energy Transfer Dynamics in Molecular Systems*, 3rd edn. (Wiley-VCH, Weinheim, 2011)
6. M. Mohseni, Y. Omar, G.S. Engel, M.B. Plenio, *Quantum Effects in Biology* (Cambridge University Press, Cambridge, 2014)
7. U. Weiss, *Quantum Dissipative Systems*, 4th edn. (World Scientific, Hackensack, 2012)
8. M. Vojta, N.-H. Tong, R. Bulla, Quantum phase transitions in the sub-ohmic spin-boson model: failure of the quantum-classical mapping. *Phys. Rev. Lett.* **94**(7), 070604 (2005)
9. A. Winter, H. Rieger, M. Vojta, R. Bulla, Quantum phase transition in the sub-ohmic spin-boson model: quantum Monte Carlo study with a continuous imaginary time cluster algorithm. *Phys. Rev. Lett.* **102**(3), 030601 (2009)
10. D. Kast, J. Ankerhold, Persistence of coherent quantum dynamics at strong dissipation. *Phys. Rev. Lett.* **110**, 010402 (2013). <https://doi.org/10.1103/PhysRevLett.110.010402>
11. M. Xu, Y. Yan, Q. Shi, J. Ankerhold, J.T. Stockburger, Taming quantum noise for efficient low temperature simulations of open quantum systems. *Phys. Rev. Lett.* **129**, 230601 (2022). <https://doi.org/10.1103/PhysRevLett.129.230601>
12. H.-D. Zhang, Y.-J. Yan, Kinetic rate kernels via hierarchical Liouville-space projection operator approach. *J. Phys. Chem. A* **120**, 3241–3245 (2016)
13. M. Xu, L. Song, K. Song, Q. Shi, Convergence of high order perturbative expansions in open system quantum dynamics. *J. Chem. Phys.* **146**(6), 064102 (2017)
14. M. Xu, Y. Yan, Y. Liu, Q. Shi, Convergence of high order memory kernels in the Nakajima-Zwanzig generalized master equation and rate constants: case study of the spin-boson model. *J. Chem. Phys.* **148**(16), 164101 (2018)
15. F. Shibata, T. Arimitsu, Expansion formulas in nonequilibrium statistical mechanics. *J. Phys. Soc. Jpn.* **49**(3), 891–897 (1980)
16. R.H. Terwiel, Projection operator method applied to stochastic linear differential equations. *Physica* **74**(2), 248–265 (1974)
17. Z. Gong, Z. Tang, S. Mukamel, J. Cao, J. Wu, A continued function resummation form of bath relaxation effect in the spin-boson model. *J. Chem. Phys.* **142**, 084103 (2015)
18. M. Aihara, H.M. Sevian, J.L. Skinner, Non-Markovian relaxation of a spin-1/2 particle in a fluctuating transverse field: cumulant expansion and stochastic simulation results. *Phys. Rev. A* **41**, 6596 (1990)
19. Y. Tanimura, R. Kubo, Time evolution of a quantum system in contact with a nearly Gaussian–Markoffian noise bath. *J. Phys. Soc. Jpn.* **58**, 101 (1989)
20. Y. Tanimura, Stochastic Liouville, Langevin, Fokker–Planck, and master equation approaches to quantum dissipative systems. *J. Phys. Soc. Jpn.* **75**, 082001–082039 (2006)
21. Y. Tanimura, Numerically “exact” approach to open quantum dynamics: the hierarchical equations of motion (HEOM). *J. Chem. Phys.* **153**(2), 020901 (2020)
22. H.-D. Zhang, L. Cui, H. Gong, R.-X. Xu, X. Zheng, Y. Yan, Hierarchical equations of motion method based

- on Fano spectrum decomposition for low temperature environments. *J. Chem. Phys.* **152**(6), 064107 (2020)
23. C.-Y. Hsieh, J. Cao, A unified stochastic formulation of dissipative quantum dynamics. I. Generalized hierarchical equations. *J. Chem. Phys.* **148**(1), 014103 (2018)
 24. Q. Wang, Z. Gong, C. Duan, Z. Tang, J. Wu, Dynamical scaling in the ohmic spin-boson model studied by extended hierarchical equations of motion. *J. Chem. Phys.* **150**(8), 084114 (2019)
 25. Q. Shi, L.-P. Chen, G.-J. Nan, R.-X. Xu, Y.-J. Yan, Efficient hierarchical Liouville-space propagator to quantum dissipative dynamics. *J. Chem. Phys.* **130**, 084105–084108 (2009)
 26. H. Liu, L. Zhu, S. Bai, Q. Shi, Reduced quantum dynamics with arbitrary bath spectral densities: hierarchical equations of motion based on several different bath decomposition schemes. *J. Chem. Phys.* **140**, 134106 (2014)
 27. Q. Shi, Y. Xu, Y. Yan, M. Xu, Efficient propagation of the hierarchical equations of motion using the matrix product state method. *J. Chem. Phys.* **148**(17), 174102 (2018)
 28. L. Han, V. Chernyak, Y.-A. Yan, X. Zheng, Y. Yan, Stochastic representation of non-Markovian fermionic quantum dissipation. *Phys. Rev. Lett.* **123**, 050601 (2019). <https://doi.org/10.1103/PhysRevLett.123.050601>
 29. Y.-A. Yan, H. Wang, J. Shao, A unified view of hierarchy approach and formula of differentiation. *J. Chem. Phys.* **151**(16), 164110 (2019)
 30. A. Erpenbeck, C. Hertlein, C. Schinabeck, M. Thoss, Extending the hierarchical quantum master equation approach to low temperatures and realistic band structures. *J. Chem. Phys.* **149**(6), 064106 (2018)
 31. H. Rahman, U. Kleinekathöfer, Chebyshev hierarchical equations of motion for systems with arbitrary spectral densities and temperatures. *J. Chem. Phys.* **150**(24), 244104 (2019)
 32. Y. Yan, T. Xing, Q. Shi, A new method to improve the numerical stability of the hierarchical equations of motion for discrete harmonic oscillator modes. *J. Chem. Phys.* **153**(20), 204109 (2020)
 33. T. Ikeda, G.D. Scholes, Generalization of the hierarchical equations of motion theory for efficient calculations with arbitrary correlation functions. *J. Chem. Phys.* **152**(20), 204101 (2020)
 34. K. Nakamura, Y. Tanimura, Hierarchical Schrödinger equations of motion for open quantum dynamics. *Phys. Rev. A* **98**, 012109 (2018). <https://doi.org/10.1103/PhysRevA.98.012109>
 35. R. Härtle, G. Cohen, D.R. Reichman, A.J. Millis, Decoherence and lead-induced interdot coupling in nonequilibrium electron transport through interacting quantum dots: a hierarchical quantum master equation approach. *Phys. Rev. B* **88**, 235426 (2013)
 36. I.S. Dunn, R. Tempelaar, D.R. Reichman, Removing instabilities in the hierarchical equations of motion: exact and approximate projection approaches. *J. Chem. Phys.* **150**(18), 184109 (2019)
 37. Y.-A. Yan, J. Shao, Stochastic description of quantum Brownian dynamics. *Front. Phys.* **11**(4), 1–24 (2016)
 38. Y. Ke, R. Borrelli, M. Thoss, Hierarchical equations of motion approach to hybrid fermionic and bosonic environments: matrix product state formulation in twin space. *J. Chem. Phys.* **156**(19), 194102 (2022)
 39. X. Li, Y. Su, Z.-H. Chen, Y. Wang, R.-X. Xu, X. Zheng, Y. Yan, Dissipations as generalized Brownian particles for open quantum systems: dissipaton-embedded quantum master equation. arXiv preprint [arXiv:2303.10666](https://arxiv.org/abs/2303.10666) (2023)
 40. Y. Yan, M. Xu, T. Li, Q. Shi, Efficient propagation of the hierarchical equations of motion using the tucker and hierarchical tucker tensors. *J. Chem. Phys.* **154**(19), 194104 (2021)
 41. T. Li, Y. Yan, Q. Shi, A low-temperature quantum Fokker–Planck equation that improves the numerical stability of the hierarchical equations of motion for the Brownian oscillator spectral density. *J. Chem. Phys.* **156**, 064107 (2022)
 42. Y. Ke, Tree tensor network state approach for solving hierarchical equations of motions. arXiv preprint [arXiv:2304.05151](https://arxiv.org/abs/2304.05151) (2023)
 43. Z.-H. Chen, Y. Wang, X. Zheng, R.-X. Xu, Y. Yan, Universal time-domain Prony fitting decomposition for optimized hierarchical quantum master equations. *J. Chem. Phys.* **156**, 221102 (2022)
 44. T.P. Fay, A simple improved low temperature correction for the hierarchical equations of motion. *J. Chem. Phys.* **157**(5), 054108 (2022)
 45. Y.-J. Yan, Theory of open quantum systems with bath of electrons and phonons and spins: many-dissipaton density matrixes approach. *J. Chem. Phys.* **140**, 054105 (2014)
 46. X. Dan, M. Xu, J. Stockburger, J. Ankerhold, Q. Shi, Efficient low temperature simulations for fermionic reservoirs with the hierarchical equations of motion method: application to the Anderson impurity model. arXiv preprint [arXiv:2211.04089](https://arxiv.org/abs/2211.04089) (2022)
 47. D. Tamascelli, A. Smirne, S.F. Huelga, M.B. Plenio, Nonperturbative treatment of non-Markovian dynamics of open quantum systems. *Phys. Rev. Lett.* **120**(3), 030402 (2018)
 48. D. Suess, A. Eisfeld, W.T. Strunz, Hierarchy of stochastic pure states for open quantum system dynamics. *Phys. Rev. Lett.* **113**(15), 150403 (2014)
 49. E. Arrigoni, M. Knap, W. Von Der Linden, Nonequilibrium dynamical mean-field theory: an auxiliary quantum master equation approach. *Phys. Rev. Lett.* **110**(8), 086403 (2013)
 50. A.J. Leggett, S. Chakravarty, A.T. Dorsey, M.P.A. Fisher, A. Garg, W. Zwerger, Dynamics of the dissipative two-level system. *Rev. Mod. Phys.* **59**, 1 (1987)
 51. Y. Tanimura, Reduced hierarchical equations of motion in real and imaginary time: correlated initial states and thermodynamic quantities. *J. Chem. Phys.* **141**, 044114 (2014)
 52. L.Z. Song, Q. Shi, Calculation of correlated initial state in the hierarchical equations of motion method using an imaginary time path integral approach. *J. Chem. Phys.* **143**, 194106 (2015)
 53. R.P. Feynman, F.L. Vernon, The theory of a general quantum system interacting with a linear dissipative system. *Ann. Phys.* **24**, 118 (1963)
 54. L. Mühlbacher, J. Ankerhold, C. Escher, Path-integral Monte Carlo simulations for electronic dynamics on

- molecular chains. i. Sequential hopping and super exchange. *J. Chem. Phys.* **121**(24), 12696–12707 (2004)
55. Y. Nakatsukasa, O. Sète, L.N. Trefethen, The AAA algorithm for rational approximation. *SIAM J. Sci. Comput.* **40**(3), 1494–1522 (2018)
 56. M. Xu, V. Vadimov, M. Krug, J. Stockburger, J. Ankerhold, A universal framework for quantum dissipation: minimally extended state space and exact time-local dynamics. arXiv preprint [arXiv:2307.16790](https://arxiv.org/abs/2307.16790) (2023)
 57. R.-X. Xu, P. Cui, X.-Q. Li, Y. Mo, Y.-J. Yan, Exact quantum master equation via the calculus on path integrals. *J. Chem. Phys.* **122**, 041103 (2005)
 58. M. Xu, J.T. Stockburger, J. Ankerhold, Heat transport through a superconducting artificial atom. *Phys. Rev. B* **103**, 104304 (2021). <https://doi.org/10.1103/PhysRevB.103.104304>
 59. M. Xu, J. Stockburger, G. Kurizki, J. Ankerhold, Minimal quantum thermal machine in a bandgap environment: non-Markovian features and anti-Zeno advantage. *New. J. Phys.* **24**(3), 035003 (2022)
 60. Y. Yan, Y. Liu, T. Xing, Q. Shi, Theoretical study of excitation energy transfer and nonlinear spectroscopy of photosynthetic light-harvesting complexes using the nonperturbative reduced dynamics method. *Wiley Interdiscip. Rev. Comput. Mol. Sci.* **11**(3), 1498 (2021)
 61. C. Lubich, I. Oseledets, B. Vandereycken, Time integration of tensor trains. *SIAM J. Num. Anal.* **53**, 917–941 (2015)
 62. H.P. Breuer, F. Petruccione, *The Theory of Open Quantum Systems* (Oxford University Press, New York, 2002)
 63. F.L. Traversa, M. Di Ventura, F. Bonani, Generalized Floquet theory: application to dynamical systems with memory and Bloch's theorem for nonlocal potentials. *Phys. Rev. Lett.* **110**(17), 170602 (2013)
 64. L. Magazzù, S. Denisov, P. Hänggi, Asymptotic Floquet states of non-Markovian systems. *Phys. Rev. A* **96**(4), 042103 (2017)
 65. L. Magazzù, S. Denisov, P. Hänggi, Asymptotic Floquet states of a periodically driven spin-boson system in the nonperturbative coupling regime. *Phys. Rev. E* **98**(2), 022111 (2018)
 66. A. Trushechkin, Higher-order corrections to the redfield equation with respect to the system-bath coupling based on the hierarchical equations of motion. *Lobachevskii J. Math.* **40**(10), 1606–1618 (2019)
 67. H.-P. Breuer, E.-M. Laine, J. Piilo, B. Vacchini, Colloquium: Non-Markovian dynamics in open quantum systems. *Rev. Mod. Phys.* **88**, 021002 (2016). <https://doi.org/10.1103/RevModPhys.88.021002>
 68. H. Dekker, Noninteracting-blip approximation for a two-level system coupled to a heat bath. *Phys. Rev. A* **35**, 1436 (1987)